Post Launch Study Report

of

VAS-E Performance

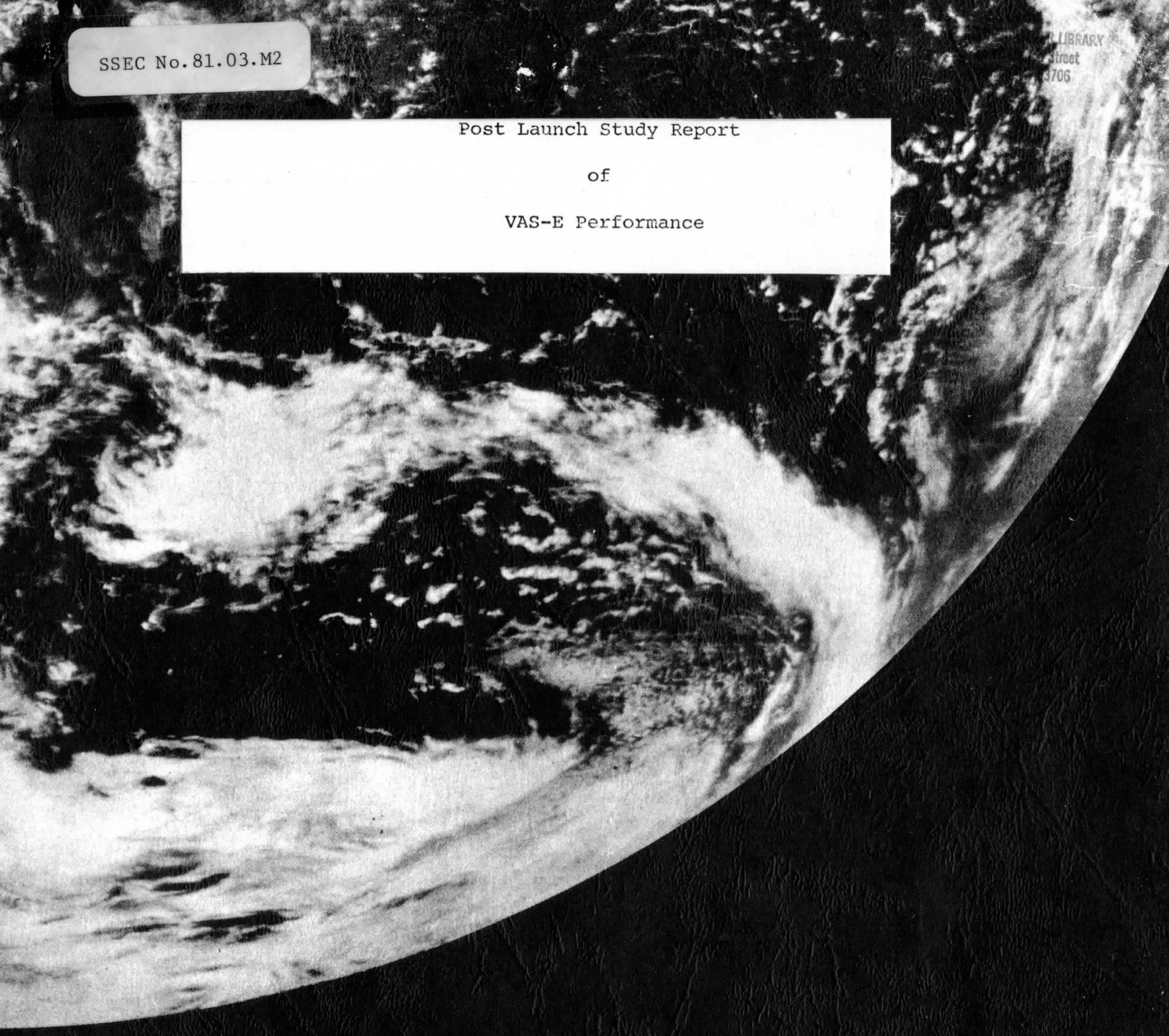

A REPORT

from the space science and engineering center
the university of wisconsin-madison
madison, wisconsin

Post Launch Study Report

of

VAS-E Performance

A Report Under NASA Contract

NAS5-21965

by

Paul Menzel

March 1981

The University of Wisconsin
Space Science and Engineering Center
1225 West Dayton Street
Madison, Wisconsin 53706

INTRODUCTION

The GOES-E spacecraft, carrying the VAS-E instrument, was successfully launched May 22, 1981. It arrived on station at 85° west longitude two weeks later and then began transmitting engineering checkout and sounding data. On August 5, 1981 it was placed at 75° west longitude and became the operational east GOES.This report is based on the analyses of the inflight data and is an update of the Prelaunch Study Report of VAS-E Performance. Many of the analyses performed for VAS-D have been repeated for VAS-E; the theoretical basis for these calculations can be found in the VAS-D prelaunch and postlaunch study reports and will not be repeated here.

I. INFLIGHT VAS-E CALIBRATION

Electronic Calibration

Tables I.1 and I.2 summarize the inflight measurements of the electronic calibration waveform. The average ramp slope was found to be .309 volt/msec (within 1% of the specified value .312 volt/msec and the same as the VAS-D ramp slope) and the average plateau voltage was determined to be 4.44 volts (within 1.5% of the specified value 4.50 volts). The data confirms that all detectors are functioning properly. The observed noise level for band 8 is somewhat lower than the other bands while for band 9 it is higher.

Radiometric Calibration

Comparisons of VAS radiances and HIRS estimates through regression relations of VAS radiances were made, as described in the VAS-D postlaunch report. Radiances from VAS-E gathered on July 20, 1981 from 1502 GMT and September 23, 1981 from 1433 GMT are compared with NOAA-6 data from 1420 GMT and 1442 GMT of the same days respectively. As before, VAS radiances for clear fields of view over uniform areas (plain regions, cloudless water) were estimated from viewing angle corrected HIRS radiances close in time (within 60 minutes). Table I.3 shows the comparison of VAS radiances and VAS radiance estimates from HIRS for the twelve VAS spectral bands (the brightness temperatures of the Planck radiances are recorded). Since the window bands 7, 8, and 12 are most sensitive to good navigation and time coincidence, the results for these bands should be viewed cautiously. Band 12 also includes reflected solar contributions which cannot easily be corrected. The general agreement between VAS-E and the HIRS is quite good, just as was witnessed with VAS-D. The relative errors for VAS-E are somewhat

Table I.1 VAS-E Electronic Calibration Ramp

filter	detector	ramp slope (volts/msec)	offset (volts)	linear regression coefficient	σ ramp (volts)
8	Upper Large HgCdTe	.306	-.655	.9993	.040
8	Lower Large HgCdTe	.309	-.630	.9987	.057
8	Upper Small HgCdTe	.313	-.760	.9999	.005
8	Lower Small HgCdTe	.309	-.734	.9999	.005
12	Upper Large InSb	.308	-.666	.9993	.042
12	Lower Larger InSb	.307	-.629	.9987	.057
9	Upper Large HgCdTe	.310	-.770	.9994	.040
9	Lower Large HgCdTe	.307	-.689	.9992	.045
9	Upper Small HgCdTe	.310	-.759	.9969	.088
9	Lower Small HgCdTe	.305	-.640	.9968	.089
4	Upper Large HgCdTe	.312	-.781	.9999	.012
4	Lower Large HgCdTe	.311	-.744	.9999	.013
4	Upper Small HgCdTe	.310	-.741	.9997	.026
4	Lower Small HgCdTe	.309	-.747	.9998	.023
11	Upper Large InSb	.301	-.646	.9993	.042
11	Lower Large InSb	.308	-.631	.9987	.057

Table I.2 VAS-E Electronic Calibration Plateaus

filter	detector	zero (volts)		offset (volts)		plateau (volts)	
		$\bar{z}$	σ_z	$\bar{o}$	σ_o	$\bar{p}$	σ_p
8	ULH	.006	.015	.255	.002	4.405	.003
8	LLH	.015	.021	.264	.003	4.475	.003
8	USH	.007	.004	.262	.004	4.489	.010
8	LSH	.004	.004	.258	.004	4.421	.004
12	ULI	.003	.010	.249	.016	4.421	.018
12	LLI	.019	.023	.268	.015	4.440	.011
9	ULH	.020	.029	.244	.040	4.439	.057
9	LLH	.086	.043	.354	.049	4.458	.034
9	USH	.038	.049	.284	.075	4.434	.083
9	LSH	.101	.074	.262	.083	4.423	.084
4	ULH	.003	.005	.260	.012	4.470	.041
4	LLH	.021	.011	.278	.014	4.473	.018
4	USH	.019	.021	.274	.027	4.473	.026
4	LSH	.011	.018	.252	.030	4.416	.019
11	ULI	.009	.013	.256	.019	4.332	.015
11	LLI	.020	.022	.255	.015	4.447	.015

Table I.3 VAS Radiances (Brightness Temperatures Compared to VAS Radiance (Brightness Temperature) Estimates from TIROS Data

$B^{-1}(R_v^{est}) - B^{-1}(R_v)$

VAS Bands #	VAS Bands (cm^{-1})	HIRS Bands # [a]	HIRS Bands (cm^{-1})	July 20, 1981 [b] abs (°C)	July 20, 1981 [b] rel (°C)	September 23, 1981 abs (°C)	September 23, 1981 rel (°C)
1	679	2	679	1.54	.72	.33	1.15
2	691	3	691	.84	.71	.33	.76
3	702	4	704	.15	.36	-.11	.59
4	714	5	716	-.40	.33	-.90	.57
5	750	7	748	-1.13	.83	-.78	.63
6	2210	14	2212	-1.38	.43	-.70	.80
7	790	10	1217[c]	-.73	.95	.91	1.44
8	895	8	900	2.56	.67	3.88	1.43
9	1377	11	1363	-3.44	.83	-2.95	.96
10	1487	12	1484	-3.82	.96	-3.74	.95
11	2250	15	2240	-.12	1.02	-	-[d]
12	2535	18	2511	-3.25	1.03	-1.50	1.60

[a] The HIRS band closest to the VAS band is listed; all HIRS bands enter in the determination of R_v^{est} through the regression relation.

[b] The number of comparisons made are 26 and 33 respectively for July 20 and September 23.

[c] The transmittance of HIRS band 10 is similar to that of VAS band 7 although the frequencies are different.

[d] Band 11 comparisons are unavailable on this day.

smaller than for VAS-D while the offsets for the water vapor bands 9 and 10 are noticeably larger. The VAS-D bias in bands 2 through 4 is not seen here for VAS-E.

The VAS radiances were also compared to the LFM analysis of radiosonde data over a period of several months. Table I.4 shows this comparison. Data for the window bands are not presented because no reliable surface analysis was available; band 11 is unreliable and not presented because the spin budget was reduced drastically and the noise reduction for this band was not accomplished. The relative errors are around 1.0°C except for the noisy bands 1, 2, and 9 and are within the expected accuracy of the comparison. In this analysis no discernible bias was detected in any of the twelve spectral bands (nor has any bias been used in our VAS-E sounding retrieval algorithms)! This contrasts sharply with the documented VAS-D biases; also the relative errors for VAS-E are noticeably smaller than those of VAS-D in a similar earlier analysis.

Table I.4 VAS Radiances (Brightness Temperatures) Compared to Radiances (Brightness Temperatures) Determined from LFM Analysis of Radiosonde Data

Band	$B^{-1}(R_{LFM}) - B^{-1}(R_V)$	
	abs (°C)	rel (°C)
1	.0	2.8
2	.0	1.4
3	.0	1.0
4	.0	.9
5	.0	.6
6	.0	.7
7	-	-
8	-	-
9	.0	1.5
10	.0	.7
11	-	-
12	-	-

II. INFLIGHT VAS-D DETECTOR NOISE REDUCTION ANALYSIS

Figure II.1 shows the autocovariance of noise as a function of sampling interval in the large detectors derived from inflight data and from prelaunch test data. The comparison shows the inflight autocovariance to be somewhat smaller than that expected from prelaunch calculations. However the effect on the spin budget inflight was not noticeable. The spin budget summary of the findings during the postlaunch checkout on June 9, 1981 are found in Table II.1. Subsequent noise reduction analysis on July 14, 1981 reconfirmed the initial conclusions; the spin budget had not changed from 39 spins.

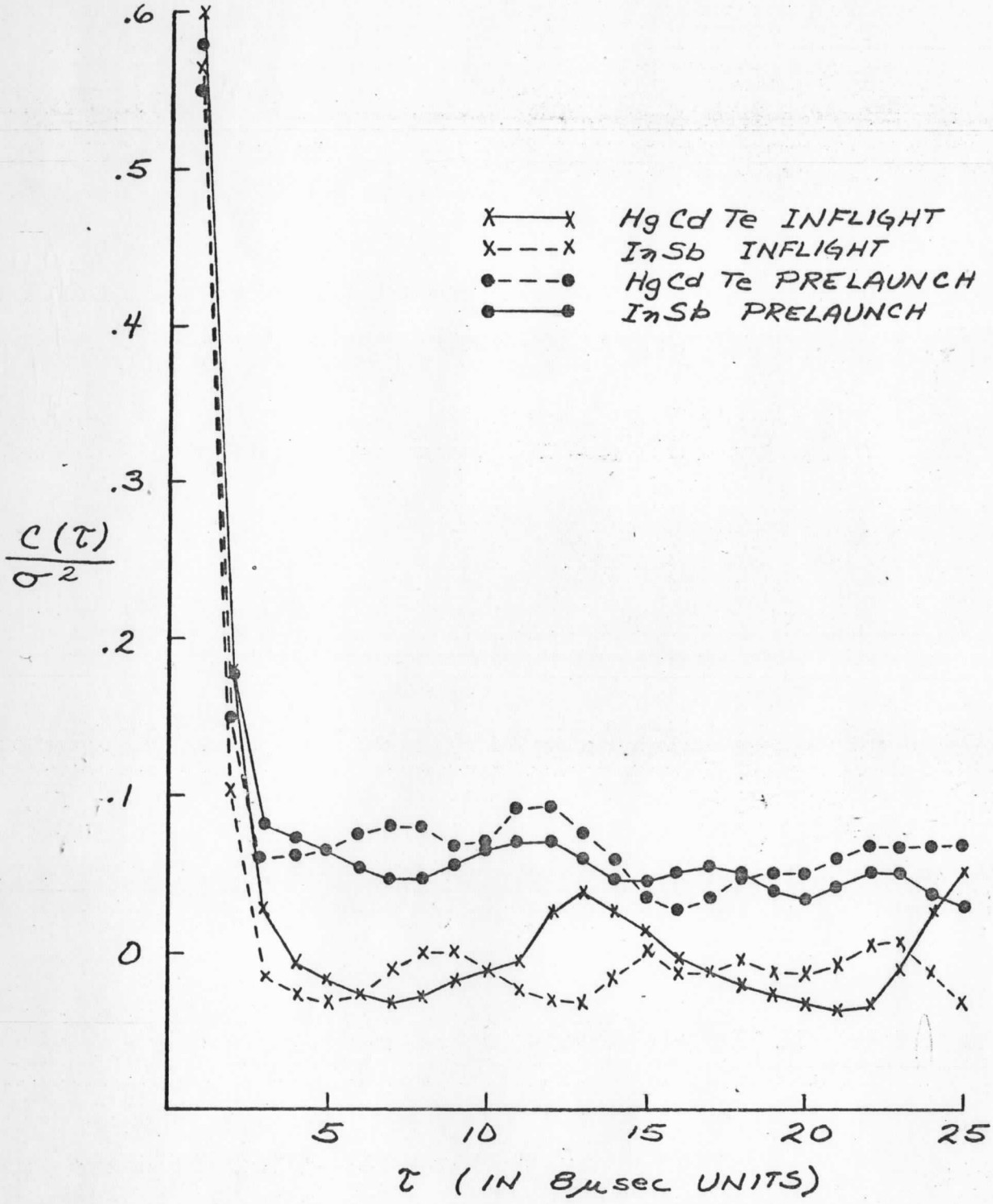

FIGURE II.1 VAS-E AUTOCOVARIANCE OF NOISE $C(\tau)/\sigma^2$ AS A FUNCTION OF SAMPLING INTERVAL τ IN THE LARGE DETECTORS EVALUATED FROM PRELAUNCH TEST DATA AND FROM INFLIGHT DATA.

Table II.1 Inflight Spin Budget of VAS-E Large Detectors

Band	Single Sample Noise (erg/etc)		Spin Budget*	
	inflight	prelaunch	inflight	prelaunch
1	2.	3.00	1	2
2	1.42	1.52	7	7
3	1.22	1.11	4	4
4	1.04	.99	3	3
5	.83	.84	3	2
6	.026	.025	6	7
7	.64	.70	2	2
8	.09	.10	1	1
9	.61	.68	4	4
10	.15	.15	1	1
11	.026	.026	6	8
12	.007	.008	1	1
			39	42

*for sounding in 30 x 30 km area, except 150 x 150 km area for band 1.

III. INFLIGHT DETERMINATION OF MISREGISTRATION OF VAS-E IMAGES

Preliminary determinations of the misregistration of images of the IR window channels (band 8 using HgCdTe detectors, band 12 using InSb detectors) and the visible channel were made from December, 1981 images of Baja, California. As with VAS-D it was found that the IR image is east and south of the visible image. Table III.1 summarizes these findings.

Table III.1 Misregistration of VAS-E Images

East West

A \ B	Visible	HgCdTe(L)	HgCdTe(S)	InSb
Visible	-	.34	.34	.34
HgCdTe(L)	-.34	-	0	0
HgCdTe(S)	-.34	0	-	0
InSb	-.34	0	0	-

Image A is X milliradians west of Image B

North South

A \ B	Visible	HgCdTe(L)	HgCdTe(S)	InSb
Visible	-	.16	.16	.16
HgCdTe(L)	-.16	-	0	0
HgCdTe(S)	-.16	0	-	0
InSb	-.16	0	0	-

Image A is X milliradians north of Image B